

Durham Research Online

Deposited in DRO:

15 March 2011

Version of attached file:

Published Version

Peer-review status of attached file:

Peer-reviewed

Citation for published item:

Zheng, G. and Clark, S.J. and Brand, S. and Abram, R.A. (2006) 'Lattice dynamics of polyaniline and poly(p-pyridyl vinylene) : first-principles determination.', *Physical review B.*, 74 (16). p. 165210.

Further information on publisher's website:

<http://dx.doi.org/10.1103/PhysRevB.74.165210>

Publisher's copyright statement:

2006 The American Physical Society

Additional information:

Use policy

The full-text may be used and/or reproduced, and given to third parties in any format or medium, without prior permission or charge, for personal research or study, educational, or not-for-profit purposes provided that:

- a full bibliographic reference is made to the original source
- a [link](#) is made to the metadata record in DRO
- the full-text is not changed in any way

The full-text must not be sold in any format or medium without the formal permission of the copyright holders.

Please consult the [full DRO policy](#) for further details.

Lattice dynamics of polyaniline and poly(*p*-pyridyl vinylene): First-principles determinationG. Zheng,^{1,2,*} S. J. Clark,² S. Brand,² and R. A. Abram²¹*School of Mathematics and Physics, China University of Geosciences (Wuhan), 430074, China*²*Department of Physics, University of Durham, Durham DH1 3LE, United Kingdom*

(Received 14 July 2006; published 26 October 2006)

First-principles density functional studies of the dynamical properties of the conjugated polymers polyaniline and poly(*p*-pyridyl vinylene) are presented in this work. We have employed linear response within density functional perturbation theory, as implemented in the CASTEP code, to investigate the Born effective charges, polarizabilities, and vibrational properties. With regard to the last, we have calculated the vibrational frequencies and made assignments of the modes for the two polymers. Most of the phonon modes have been classified and we have shown that the higher frequency modes are associated with C—H and C=N stretching modes. We also present the results of calculations of the polarizability and permittivity of the materials which are in reasonable agreement with the typical values of conjugated polymers. Dynamical Born effective charges have been calculated and compared with the Mulliken population atomic charges. It is found that notable differences exist between the Born effective charges for the nitrogen atoms in the conducting polymers, and we conclude that effective charges are more appropriate for use in the study of the dynamics of the systems. Differences are found in the ir absorption spectra obtained for the two polymers, which can be attributed to the structural differences of the two materials. It is found that the presence of the nitrogen atom plays an important role in determining their lattice dynamics.

DOI: [10.1103/PhysRevB.74.165210](https://doi.org/10.1103/PhysRevB.74.165210)

PACS number(s): 71.15.Mb, 71.20.Rv, 82.20.Wt

I. INTRODUCTION

Conjugated polymers have attracted considerable interest in fundamental and applied research since the discovery of substantial conductivity in doped polymers.^{1,2} In particular, a great deal of effort has been devoted to understanding the electronic and dynamical properties of conjugated polymers. Polyaniline (PANi) and poly(*p*-pyridyl vinylene)(PPyV) are conducting polymers which differ from their undoped counterparts such as poly(*p*-phenylene vinylene) (PPV) in that they have a nitrogen heteroatom. They are straightforward to synthesize and in addition they have excellent environmental and thermal stability.³ Further, the materials are easy to process and there are quite a large number of possible substitutions which give the opportunity to tune the electrical and optical properties. The wide range of controllable optoelectronic properties, coupled with excellent stability, make them attractive as electronic materials for potential use in a variety of applications such as biosensors,⁴ batteries,⁵ and field effect transistors.^{6–8}

Experimental and theoretical investigations of the dynamical properties of conjugated polymers play a key role in understanding the structural and microscopic optoelectronic properties of the materials in various phases in both the pristine and doped states.^{9,10} However, it is often the case that information obtained by different methods has been quite inconsistent.¹¹ Though there have been a number of studies of the electronic and dynamic properties of PANi and PPyV, no consensus has been reached on the assignment of the vibrational modes. For example, experimental infrared (ir) mode frequencies have been published for PANi,^{12–14} but one paper did not assign most of the observed modes,¹³ and another assigned only the fundamental ones.¹⁴ Using a harmonic potential with parameters transferred from other molecules, Kostić *et al.*¹⁵ calculated the vibrational modes,

which are in quite good agreement with previously published data. However, despite these results, no comprehensive study is available concerning the dynamical properties of the materials, especially the dynamical anisotropy. Realistic first-principles calculations are a way forward but they are computationally very demanding and it is often the case that the calculations of the dynamical properties are of the average axial values for simple polymers only,^{16,17} while ignoring the anisotropy information. Nevertheless, some progress has been made in understanding the anisotropy of the polarizability for molecules and molecular crystals^{18–21} and for the dielectric and vibrational properties of some of the simpler amino acid molecules.²² Very recently, an *ab initio* dynamics study has been carried out for the undoped polymer PPV.²³

In this work we present a first-principles investigation of the dynamical properties of the conducting polymers PANi and PPyV. We first study the vibrational properties of the conducting materials; then we concentrate on the electric field response and Born effective and Mulliken charges. The remainder of this paper is organized as follows. Sections II and III present the theory and computational details, and then in Sec. IV we present and discuss the calculated results for the materials. A short summary concludes the paper in Sec. V.

II. THEORY

Only a brief outline is given here, but more details of the theory of the lattice dynamics and perturbations of systems with electric fields can be found elsewhere.^{24–26} When an electric field ϵ is applied to a polymer system, the change of the dipole moment \mathbf{d} may be expressed as

$$d_i - d_{0i} = \alpha_{ij}\epsilon_j + \gamma_{ijk}\epsilon_j\epsilon_k + \dots, \quad (1)$$

where i, j , and k run over the x, y , and z axes of the system, \mathbf{d}_0 is the dipole moment at zero field, and ϵ_j, ϵ_k are the j th

and k th components of the field ϵ , respectively. α_{ij} is the polarizability tensor and γ_{ijk} the first-order hyperpolarizability. The polarizability tensor components α_{ij} can be obtained by finding the second-order derivatives of the total energy E of the system:

$$\alpha_{ij} = \frac{\partial^2 E}{\partial \epsilon_i \partial \epsilon_j}. \quad (2)$$

In this work we calculate the polarizability components by the use of linear response, within density functional perturbation theory (DFPT).^{24,25} DFPT is not only one of the most robust methods for the calculation of dynamic properties, but it is also a method that naturally enables the calculation of the second-order derivatives of the total energy, and thus dynamical quantities, such as the polarizability, to be evaluated directly. It is also possible to calculate a number of other properties by considering different perturbations. For example, a perturbation of the ionic positions can be used to obtain the dynamical matrix and information on the vibrational properties.

The polarizability can also be obtained using the finite-difference (FD) method, where appropriate. In the FD method, the dipole moment as a function of electric field is obtained and then the polarizability tensor components are derived as the proportionality coefficients. However, since the computational cost of the FD method is very considerable and it is not possible to use the method for mixed perturbations, we employ only DFPT for the study of the vibrational frequencies and effective charges.

The basic theory of lattice dynamics is well understood and has been described in detail by, for example, Born and Huang.²⁶ The properties of phonon modes may be described directly from the second-order derivative of the total energy with respect to atomic position. According to the harmonic approximation, for small atomic displacements from equilibrium, the total energy E_{tot} of the system may be written as²⁴

$$E_{tot} = E_{tot}^0 + \sum_{\kappa, \alpha} \sum_{\kappa', \beta} \frac{1}{2} \left(\frac{\partial^2 E_{tot}}{\partial \tau_{\kappa\alpha} \partial \tau_{\kappa'\beta}} \right) \Delta \tau_{\kappa\alpha} \Delta \tau_{\kappa'\beta} \quad (3)$$

where $\Delta \tau_{\kappa\alpha}$ is the displacement in direction α for the ion κ . The frequencies of the phonon modes ω are the eigenvalues of the eigenvalue equation,

$$\sum_{\kappa', \beta} \frac{1}{(M_{\kappa} M_{\kappa'})^{1/2}} \frac{\partial^2 E_{tot}}{\partial \tau_{\kappa\alpha} \partial \tau_{\kappa'\beta}} e(\kappa' \beta) = M_{\kappa} \omega^2 e(\kappa \alpha) \quad (4)$$

where M_{κ} is the mass of ion κ , and $e(\kappa \alpha)$ and $e(\kappa' \beta)$ are the eigenvectors.

The perturbation resulting from an applied electric field allows us to evaluate the dielectric response. In the limit of low frequencies of the applied field, the electronic dielectric permittivity tensor β_{ij} may be expressed as

$$\beta_{ij}^{\infty} = \delta_{ij} + \frac{4\pi}{\Omega_0} \alpha_{ij} \quad (5)$$

where Ω_0 is the volume of the supercell and α_{ij} is the polarizability tensor as defined in Eq. (2).

The change in the dipole moment as a result of atomic displacements may also cause changes in the polarization of the polymer system. Then the so-called Born effective charge tensor $Z_{i,jk}^*$ can be defined as²⁴

$$Z_{i,jk}^* = \Omega_0 \frac{\delta \mathcal{P}_{mac,j}}{\delta \tau_{ik}} = \frac{\delta F_{ik}}{\delta \epsilon_j} \quad (6)$$

where τ_{ik} is the k component of the position of ion i . Thus the Born effective charge tensor of the i th ion $Z_{i,jk}^*$ is the partial derivative of the macroscopic polarization with respect to a periodic displacement of that ion at the limit of zero applied electric field, and in DFPT the tensor is equivalent to that in the linear relation between the force upon an atom and the applied electric field.²⁴

It is known that the long-range behavior of the Coulomb interaction gives rise to macroscopic electric fields for longitudinal (LO) and transverse (TO) optical phonons, and the coupling between the phonon modes and the electric field gives rise to LO-TO splitting at the Γ point.^{27,28} The Born effective charge is a very important quantity and can be used to determine the well-known phenomenon of LO-TO splitting in polar semiconductors and insulators.

With knowledge of the normal modes and the Born effective charges of a system, its infrared absorption spectrum can be calculated as

$$I_m \propto \sum_{\alpha} \left| \sum_{\kappa, \beta} Z_{\kappa, \alpha\beta}^* e_m(\kappa\beta) \right|^2 \quad (7)$$

where m is the mode of vibration, $Z_{\kappa, \alpha\beta}^*$ is the effective charge, and e_m is the phonon eigenvector.

III. COMPUTATIONAL DETAILS

We have carried out our calculations with the plane-wave pseudopotential implementation of density functional theory using the CASTEP code.^{27,28} Plane-wave basis sets are advantageous compared to conventionally used localized basis sets since they are, in principle, complete and are evenly distributed in space and therefore not biased toward any individual chemical bonds. In particular, there exists only one parameter, the cutoff energy, to determine the completeness of the basis.

In our calculations, the many-body exchange and correlation interactions were described using the generalized gradient approximation proposed by Perdew and Wang,²⁹ which can provide a good description for hydrogen-bonded systems. The use of a plane-wave basis set requires periodic boundary conditions in all three dimensions. To achieve this, a periodic ‘‘supercell’’ method was used and the chain was artificially repeated in the two dimensions normal to the polymer axis with a sufficiently large unit cell to make neighboring interactions negligible. The unit cell was $10 \times 10 \times d \text{ \AA}^3$, where d is the repeat distance along the polymer chain. Norm-conserving Kleinman-Bylander³⁰ pseudopotentials were used to describe the electron-ion interactions. The cutoff energy was 1000 eV, which converges the total energy of the system to 1.0 meV/atom. The Monkhorst-Pack k -point sampling³¹ mesh of $1 \times 1 \times 8$, was employed to per-

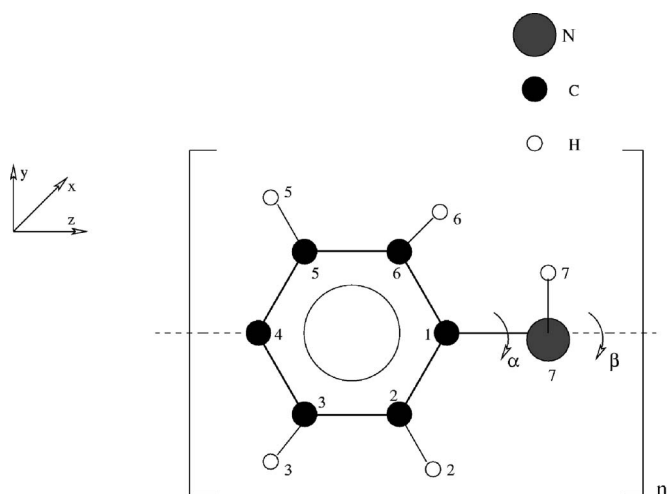


FIG. 1. The structure and numbering scheme employed for the polymer PANi. The black and white circles denote carbon (or nitrogen) and hydrogen atoms, respectively. The orientation of the polymer PANi with respect to a chosen frame of reference is shown. The polarizabilities quoted are relative to this coordinate frame. The selected optimized geometrical parameters are as follows: the repeat unit-cell length is 5.45 Å, $C_1-C_2=1.392$ Å, $C_2-C_3=1.395$ Å, $C_3-C_4=1.393$ Å, $C_4-C_5=1.396$ Å, $C_5-C_6=1.365$ Å, $C_6-C_1=1.395$ Å, $C_1-N_7=1.403$ Å. The torsion angle α is 17.5° .

form the integrations in \mathbf{k} space over the first Brillouin zone, with the grids for each cell chosen to be dense enough to also converge the total energy to 1.0 meV/atom.

We first optimized the polymer geometrical structures of the ground state using the Hellmann-Feynman force.³⁴ The resulting predicted structures of PANi and PPyV at equilibrium are shown in Figs. 1 and 2, respectively. The geometrical parameters are given in the captions of the figures, and are in good agreement with those determined by experiment.^{32,33}

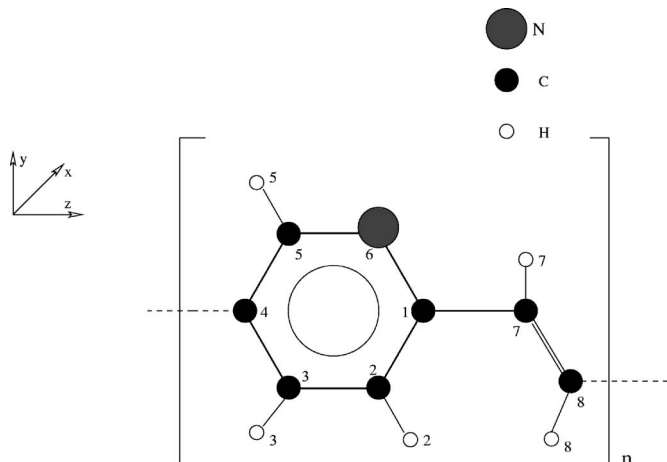


FIG. 2. The structure of the polymer PPyV. The black and white circles denote carbon (or nitrogen) and hydrogen atoms. Polarizabilities quoted are relative to this coordinate frame. The repeat unit-cell length is 6.53 Å. The bond lengths are as follows: $C_1-C_2=1.397$ Å, $C_2-C_3=1.366$ Å, $C_3-C_4=1.397$ Å, $C_4-C_5=1.399$ Å, $C_5-N_6=1.321$ Å, $N_6-C_1=1.351$ Å, $C_1-C_7=1.432$ Å, $C_7-C_8=1.346$ Å.

IV. RESULTS AND DISCUSSION

A. Vibrational frequencies

We have calculated the vibrational frequencies of the two polymers at the Γ point by using the linear response DFPT method. The calculated normal mode frequencies of the two polymers are shown in Table I. The vibrational properties of PANi have been previously studied^{35,36} in their base form and, for comparison, we also list those results in Table I. It should be pointed out that DFPT is based on the harmonic approximation and may not be valid at high temperature. As stated in Sec. I, the dynamical properties determined by different methods are often inconsistent and so it is difficult to make a direct comparison between the theoretical and experimental values. Therefore, theoretical results are predictive rather than comparative.

Table I shows that the frequencies of normal modes occur mainly in three bands. The bands in the region $225.1-419.3$ cm^{-1} for PANi and $154.7-552.3$ cm^{-1} for PPyV are due to out-of-ring-plane oscillations. The bands for PANi ranging from 604.3 to 1608.8 cm^{-1} , and from 628.4 to 1616.1 cm^{-1} for PPyV come from the “collective behavior” of the polymers, such as mixed C—C and C—N stretching, N—H and C—H bending, wagging, and rocking, etc. The bands in the region above 3000 cm^{-1} correspond to C—H and N—H stretching modes. Detailed assignments of the frequencies for both polymers are made in this work.

The vibrational properties may be used to investigate the nitrogen doping effect present in the materials. Examination of Table I indicates that the C—N (vinyl C=C) stretching modes at 1608.8 (1616.1) cm^{-1} for PANi (PPyV) are in the same range regardless of the different nitrogen doping position in the two polymers. Actually, these mode frequencies are quite stable compared with the corresponding vinyl mode 1613.7 cm^{-1} of PPV.²³ The fact that the vinyl oscillating modes occur in the same frequency range for these systems suggests that the nitrogen atom does not have much influence on them.

Given the normal modes, the infrared absorption spectra can be calculated from Eq. (7). For complex systems like conjugated conducting polymers, the ir spectra can be useful in interpreting the vibrational properties. The calculated ir spectrum for PANi is plotted in Fig. 3 and for PPyV in Fig. 4. Notable differences can be found in the predicted ir spectra for PANi, PPyV, and undoped PPV.²³ It is known that PANi and PPyV are conducting polymers; this implies that the nitrogen doping atom plays a key role in the transport mechanisms of the materials.

B. Electric field response

The linear response of the electronic charge density gives the first-order variation in the electronic density induced by the external field. Figures 5 and 6 show for PANi and PPyV the first-order electronic charge densities in response to an applied electric field obtained by using DFPT. The contributions to the charge density from different atoms can be clearly seen, and it is apparent that the polarizability is de-

TABLE I. The calculated phonon modes (in cm^{-1}) and assignments of the two polymers PANi and PPyV at the Γ point in this work. The notation is defined as follows: ν , stretching (atoms stretching in a plane or along one direction); ω , wagging (atoms shaking up and down); ρ , rocking (atoms moving from side to side). For comparison, other theoretical and experimental results are also listed in the table. Two unidentified experimental modes are also listed.

PANi				PPyV	
This work	Assignment	Calc. ^a	Expt. ^a	This work	Assignment
225.1	ρ N ₇ H ₇			154.7	ρ C ₁ C ₂ C ₇ C ₈
309.8	Phenyl ring wagging			216.8	ρ vinyl
347.2	Phenyl ring wagging			323.2	ω ring; ρ vinyl
398.0	ω H ₇ N ₇ C ₁			329.3	ω ring; ρ vinyl
419.3	ρ phenyl			412.8	ρ C ₂ C ₅ vinyl
604.3	ν N ₇ C ₁ ; ν phenyl			428.6	ω vinyl; ρ ring
612.0	ω C ₂ C ₃ C ₅ C ₆	595	611	552.3	ρ C ₁ C ₄
		637	640		
716.2	ρ N ₇ H ₇ ; ρ phenyl ring			628.4	ω ring; ρ vinyl
722.3	ν N ₇ H ₇ ; ρ phenyl ring			674.1	ω ring; ω vinyl
743.1	ν N ₇ C ₁ C ₂ C ₄ H ₂ H ₃ H ₆			736.1	ρ C ₂ C ₄ C ₈ N ₆ H ₂
767.3	ω N ₇ C ₂ C ₃ C ₄ C ₅ C ₆ H ₂			800.8	ν ring H ₂ H ₃ H ₅ H ₇ H ₈
828.6	ν N ₇ H ₇ ; phenyl ring rocking	814		818.3	ρ C ₂ C ₃ ; ρ vinyl
876.4	ω N ₇ C ₂ C ₃ C ₅ C ₆ H ₂ H ₃ H ₅ H ₆			880.0	ρ C ₄ H ₂ ; ρ vinyl
903.5	ν N ₇ H ₇ ; ω NC ₂ C ₃ C ₅ C ₆ H ₂ H ₃ H ₅ H ₆			891.9	ν ring; ν vinyl
906.6	ν N ₇ H ₇ ; ρ C ₂ C ₃ C ₅ C ₆			910.2	ρ C ₂ C ₃ C ₅ C ₈ H ₂ H ₃ H ₅ H ₇ H ₈
970.5	ω C ₂ C ₃ C ₅ C ₆ H ₂ H ₃ H ₅ H ₆	988	993	942.7	ρ vinyl
1059.1	ν C ₂ C ₃ C ₅ C ₆ H ₂ H ₃	1026	1031	947.7	ρ ring; ρ vinyl
		1083	1072		
1141.5	ν N ₇ C ₁ C ₄	1158	1157	999.9	ω C ₂ C ₃ C ₅ N ₆ H ₂ H ₃ H ₅ ; ρ vinyl
1155.4	Phenyl ring rocking	1176	1183	1088.2	ω ring; ω H ₇ H ₈
1230.1	Phenyl ring flexing	1224	1220	1160.7	ρ C ₁ C ₂ C ₃ C ₄ C ₇ C ₈ H ₂ H ₃ H ₅ H ₇ H ₈
1289.7	ν N ₇ C ₁ ; phenyl ring rocking	1289	1306	1196.4	ω C ₁ C ₂ C ₃ C ₅ H ₂ H ₃ H ₅ H ₈
1336.4	ν C ₁ C ₄	1331	1340	1253.5	ω ring; ω vinyl
1394.3	Phenyl ring wagging			1261.9	ρ ring; ω vinyl
1445.0	ρ N ₇ H ₇ ; phenyl ring rocking	1462	1456	1290.4	ρ ring; ρ vinyl
1478.0	Phenyl ring stretching	1497	1493	1331.9	ω ring; ω vinyl
1587.8	ν N ₇ C ₁ C ₄	1591	1586	1387.3	ω ring; ρ vinyl
1608.8	ν C ₁ N ₇	1612	1603	1475.0	ω ring; ν C ₇ C ₈
3012.6	ν benzene ring			1500.6	ν ring; ν vinyl
3029.6	ν C ₅ C ₆ H ₅ H ₆			1541.1	ν C ₁ C ₂ ; ν C ₃ C ₄
3044.2	ν C ₂ C ₃ H ₂ H ₃			1616.1	ν C ₇ C ₈
3058.3	ν C ₂ C ₃ H ₂ H ₃			3013.9	ν C ₈ H ₈
3344.6	ν N ₇ H ₇			3025.8	ν C ₅ H ₅
				3049.2	ν C ₃ H ₃ C ₂ H ₂
				3051.8	ν C ₇ H ₇
				3073.8	ν C ₂ H ₂

^aReference 35.

pendent on the atomic environment. Notable differences can be found in the first-order densities for the pristine aromatic polymers such as PPV,²³ and for PANi and PPyV, especially in the vicinity of the heteroatom nitrogen. Furthermore, according to Table II, the polarizabilities are strongly anisotropic with a relatively large response for an electric field applied along the z axis.

The polarizability α and permittivity β of PANi and PPyV have been calculated in this work. The coordinate systems used to define the tensors relative to a polymer chain are shown in Figs. 1 and 2. The z direction is shown in the figures, and the x and y directions are respectively perpendicular and parallel to the plane of the rings. The polarizability and permittivity tensor components calculated using

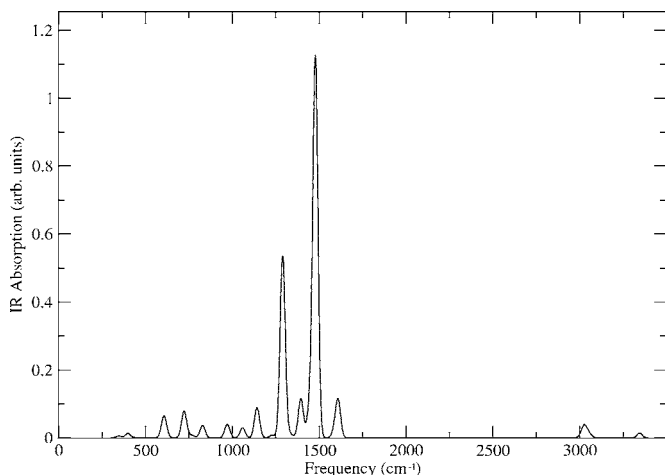


FIG. 3. Infrared absorption spectrum for PANi. Gaussian broadening has been used on the energies at $T=300$ K.

DFPT are given in Table II. For comparison, we have also calculated the polarizability for the “molecules” that are produced by saturating the two dangling bonds with hydrogen atoms in the PANi and PPyV repeat units shown in Figs. 1 and 2. The dipole moments as a function of applied field calculated by the finite-difference method are shown in Fig. 7 for the PANi “molecule.” The associated polarizability tensor components are listed in Table II along with those for PPyV. It has been previously demonstrated²¹ that the finite-difference DFT approach is capable of yielding values in good agreement with experiment for molecules.

The experimental determination of the full polarizability tensor is normally rather difficult. To the best of our knowledge, there are no reports of the anisotropy of the polarizability in the literature which we can use for comparison. However, it is perhaps useful to compare the DFPT results with the corresponding FD results. In Table II, it is found that the major contribution to the average polymer polarizability $\alpha_{av}^{DFPT} [=Tr(\alpha^{DFPT})/3]$ is the component α_{zz} . For PPyV, the three individual principal components are very similar to those of an isolated PPV chain,²³ which may be attributed to

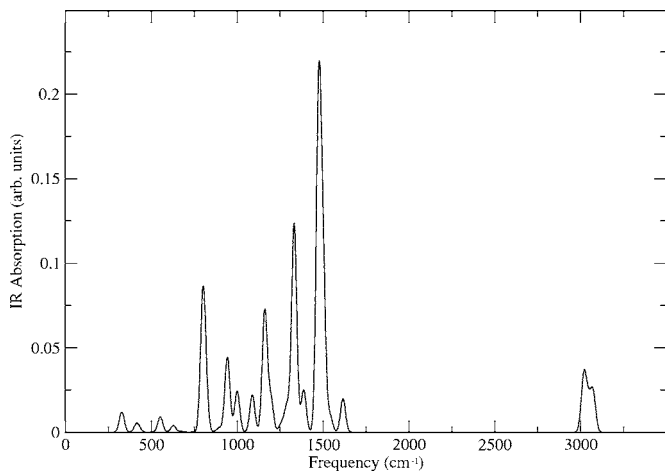


FIG. 4. The Gaussian-broadened infrared absorption spectrum for PPyV at $T=300$ K.

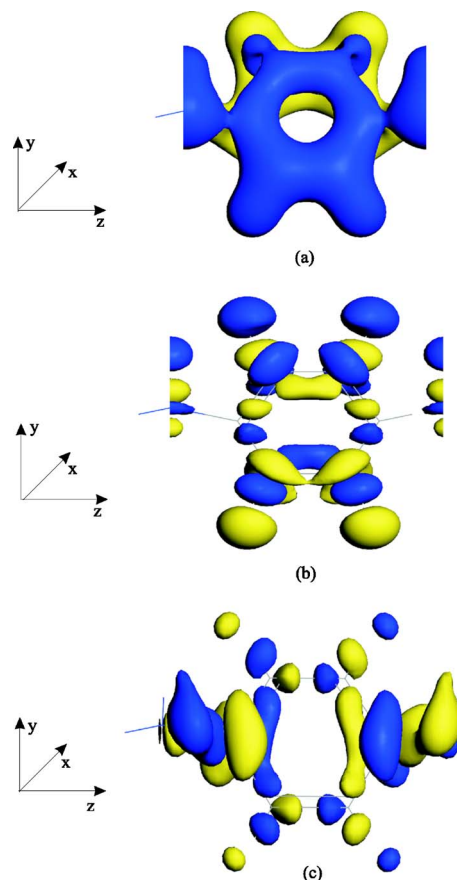


FIG. 5. (Color online) The first-order electronic charge densities for PANi. (a), (b), and (c) relate to perturbations in the x , y , and z directions, respectively. Black (blue) represents positive charge density, and gray (yellow) negative.

the similarity of the structures of PPyV and PPV. Both PPyV and PPV have the property that $\alpha_{zz} \gg \alpha_{yy}$ and $\alpha_{yy} \approx \alpha_{xx}$. The anisotropy is much greater than for α^{FD} in the case of the dangling-bond-saturated molecules. For the molecules, the component α_{zz} is less than for the polymers while α_{xx} and α_{yy} are larger. Also, α_{zz} for PANi is substantially smaller than for PPyV. It is found that the values of α_{av}^{DFPT} for the two polymers are in reasonable agreement with typical data for the axial polarizability of conjugated polymers.^{16,17}

The calculated permittivity values of PPyV also show strong anisotropy, with $\beta_{zz} \gg \beta_{yy}$ and $\beta_{xx} \approx \beta_{yy}$. The average PPyV permittivity β_{av} is 2.10 (compared to 2.15 for PPV). This feature is similar to that of PPV for an isolated polymer chain. The predicted value of PPyV β_{av} is reasonable when compared with the typical permittivity values of polymers.³⁷ Comparing the values of the permittivity tensors of the materials, it was found that the local field has a greater influence on the permittivity asymmetry of PPyV than that of PANi. For PANi, the principal components of the permittivity tensor show less anisotropy than for PPyV with $\beta_{xx} \approx \beta_{yy} \approx \beta_{zz}$, suggesting that the different doping position of the nitrogen atom is significant in this regard.

C. Born effective and Mulliken charges

We present in Table III the Born effective charges of each atom in the polymers, together with nominal atomic charges

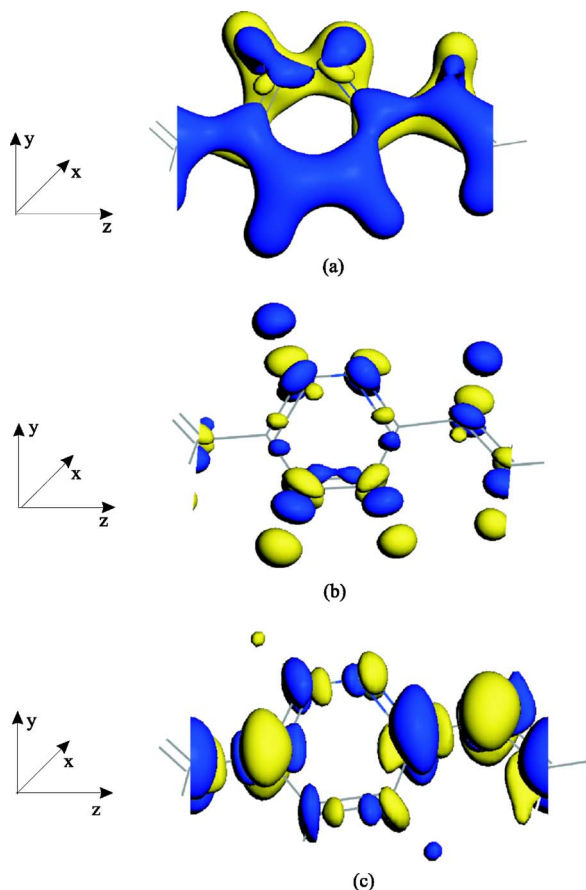


FIG. 6. (Color online) The electronic charge densities for PPyV. (a), (b), and (c) correspond to perturbations in the x , y , and z directions. Black (blue) represents positive charge density, and grey (yellow) is negative.

Z_{at} obtained by Mulliken population analyses. It is found that for the hydrogen atoms, all the Mulliken population atomic charges possess roughly the same value in both PANi and PPyV. This suggests that the electronic structure of each hydrogen atom is similar in the two polymers. For carbon atoms, except for C_1 and C_4 in PANi and C_1 , C_4 , and C_5 in PPyV, the Mulliken charges are also similar. In PANi, there is some positive charge accumulation (0.13) at the node atoms C_1 and C_4 ; for PPyV, the nominal charges for C_1 and C_4 are 0.14 and 0.16, respectively. However, perhaps due to the

TABLE II. The calculated polarizabilities α^{DFPT} and α^{FD} (in \AA^3), and permittivity β tensor components for PANi and PPyV. α_{av}^{FD} is calculated using the FD method for the two relevant molecules, which are formed by saturating the two dangling bonds with hydrogen atoms in the PANi and PPyV monomers shown in Figs. 1 and 2. For comparison, the calculated DFPT values of the two molecules are also listed in the table. α_{av} and β_{av} are $\text{Tr}(\alpha)/3$ and $\text{Tr}(\beta)/3$, respectively.

	α^{DFPT}			α_{av}^{DFPT}	Molecule	α^{FD}			α_{av}^{FD}	α^{DFPT}			α_{av}^{DFPT}	β		β_{av}
PANi	6.87	-1.18	0.00		PANi	12.8	1.2	1.5	11.5	-1.09	0.8	1.16	-0.03	0.00		
	-1.18	12.24	0.00			0.9	18.9	2.1	-1.09	17.6	0.3	-0.03	1.28	0.00		
	0.00	0.00	38.01	19.04		1.3	2.4	26.6	19.4	0.8	0.3	24.8	18.0	0.00	0.00	1.88
PPyV	7.06	-1.15	0.33		PPyV	12.3	1.6	1.1	11.9	0.6	-0.9	1.14	-0.02	0.01		
	-1.15	12.82	-1.53			1.4	28.8	0.5	0.6	26.1	1.1	-0.02	1.25	-0.03		
	0.33	-1.53	150.2	56.7		0.9	0.6	43.4	28.2	-0.9	1.1	44.5	27.5	0.01	-0.03	3.91

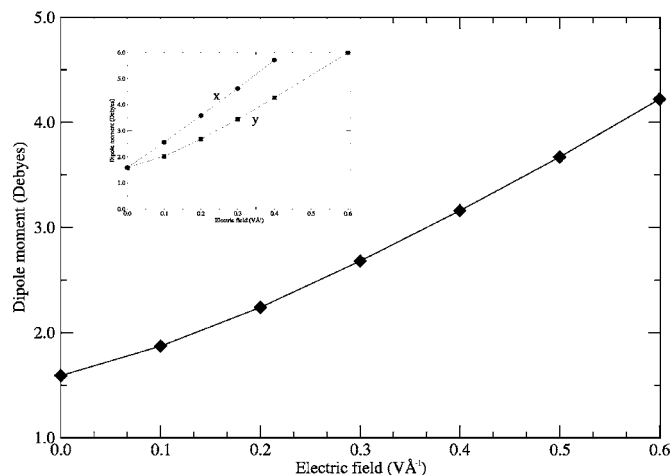


FIG. 7. The induced molecular dipole moment as a function of an external field applied in the z direction for PANi. Inset are the responses to x - and y -directed fields, respectively. The individual components of the dipole are used to fit the polarizability tensor.

nitrogen doping atom in the ring, C_5 has much less negative charge (-0.06) than its counterpart C_5 in PANi. There are marked differences between the Mulliken charges of the nitrogen atom (-0.60 versus -0.43) in PANi and PPyV, due to the fact that there is a double bond for the nitrogen atom in PPyV, and a single one in PANi.

It is instructive to make a direct comparison between the Mulliken charges and the average Born effective charges and to try to understand the reason for the discrepancies. For hydrogen atoms, there are marked differences between the average Born effective charges and the Mulliken charges. The effective charges are, with the exception of H_7 , less than one-tenth of the Mulliken charges in PANi. For the carbon atoms, there are clear differences between the two kinds of charge. In PANi, the largest discrepancy is more than 0.6, but Z_{av}^* and Z_{at} do have the same sign. In contrast, there are different charge signs for atoms C_3 , C_4 , C_5 , and C_8 in PPyV. The nitrogen doping effect in the ring may be responsible for this. The Born effective charge is directly related to the dynamic properties of a system, and especially to the electronic structure changes. Therefore the chemical environmental effects, such as neighboring chemical bonds, can play a significant role in affecting the charges. The nitrogen atom has a smaller negative effective charge (-0.685) in PPyV than that

TABLE III. The calculated Born effective charges $Z_{\alpha\beta}^*$ and nominal atomic charges Z_{at} from Mulliken population analysis for the polymers. Z_{av}^* is the average of the principal components. All the values are in units of e .

	PANi					PPyV					
	Z_{xx}^*	Z_{yy}^*	Z_{zz}^*	Z_{av}^*	Z_{at}	Z_{xx}^*	Z_{yy}^*	Z_{zz}^*	Z_{av}^*	Z_{at}	
H ₂	0.119	-0.017	0.046	0.016	0.29	H ₂	0.111	-0.004	0.010	0.039	0.28
H ₃	0.119	-0.017	0.046	0.016	0.29	H ₃	0.113	-0.031	0.047	0.043	0.29
H ₅	0.113	-0.024	-0.040	0.016	0.26	H ₅	0.085	-0.002	-0.040	0.034	0.30
H ₆	0.113	-0.024	-0.040	0.016	0.26	H ₇	0.120	-0.011	0.080	0.063	0.29
H ₇	0.209	0.088	0.176	0.158	0.31	H ₈	0.104	-0.074	0.050	0.028	0.25
C ₁	0.121	-0.051	2.246	0.772	0.13	C ₁	0.095	0.124	2.072	0.764	0.16
C ₂	-0.130	0.048	-0.164	-0.082	-0.30	C ₂	-0.087	-0.426	-1.102	-0.538	-0.28
C ₃	-0.130	0.048	-0.164	-0.082	-0.30	C ₃	-0.089	0.162	0.626	0.233	-0.26
C ₄	0.121	-0.051	2.246	0.772	0.13	C ₄	0.018	-0.262	0.007	-0.079	0.14
C ₅	-0.143	0.070	-0.437	-0.510	-0.30	C ₅	0.029	0.338	0.005	0.124	-0.06
C ₆	-0.143	0.070	-0.437	-0.510	-0.30	N ₆	-0.280	-0.433	-1.342	-0.685	-0.43
N ₇	-0.372	-0.104	-3.495	-1.324	-0.60	C ₇	-0.119	0.097	-1.029	-0.350	-0.26
						C ₈	-0.108	0.116	0.626	0.211	-0.25

(-1.324) in PANi which, as with the Mulliken charge, can be attributed to the different bonding in the two polymers. The discrepancies between the Born effective charges and Mulliken population atomic charges highlight their different origins. The Mulliken population charges are based on the partition of the Kohn-Sham orbitals and provide information on the static electronic structure, whereas the Born effective charges are based upon the dynamics of the system, and generate information concerning dynamical properties. Therefore when a dynamical system is under consideration, effective charges are normally more relevant.

V. CONCLUSION

Ab initio investigations of the dynamical properties of the two polymers PANi and PPyV have been reported. The vibrational frequencies of the polymers are calculated by directly evaluating the dynamical matrix of force constants using a linear response determination of the second-order change in the total energy induced by atomic displacements. Vibrational frequencies are calculated and assignments are made for the phonon modes of the two polymers. Most of the phonon modes have been classified: in particular the higher-frequency phonon modes are due to C—H and C=N stretch. We also present the results of calculations of the polarizability and permittivity of the materials, which are in reasonable agreement with the typical experimental values

for conjugated polymers. The calculated polarizability and permittivity tensors for the polymers in this work are in reasonable agreement with typical values of axial polarizability and permittivity of conjugated polymers where comparison is possible. Analyses of the first-order electronic charge densities give insight into the behavior of the electronic polarizability. We present the dynamical Born effective charges and the nominal Mulliken population atomic charges. It is noted that effective charges are more appropriate for use in the study of the dynamics for the system. Notable differences are found in the predicted dynamic properties obtained for PANi, PPyV, and PPV, which may play a significant role in the transport properties of this class of conducting polymers. Comments are made on their relation to the underlying polymer structure and the charge modifications induced by doping.

ACKNOWLEDGMENTS

We are grateful for an allocation of computing time on the HPC_x computer at Daresbury Laboratories through the UKCP consortium. This work was supported by an EPSRC fund (Contract No. GR/R56716/01), and by a fund for Distinguished Young Scholars of the Hubei Province of China (Contract No. 2006ABB031). The use of the computational resources at the University of Durham High Performance Computing Facility is also acknowledged. G.Z. would like to thank A. P. Monkman for helpful discussions.

- *Corresponding author. Electronic address: gzheng25@yahoo.com
- ¹C. K. Chiang, C. R. Fincher, Y. W. Park, A. J. Heeger, H. Shirakawa, E. J. Louis, S. C. Gau, and A. G. MacDiarmid, *Phys. Rev. Lett.* **39**, 1098 (1977).
- ²C. K. Chiang, M. A. Druy, S. C. Gau, A. J. Heeger, E. J. Louis, A. G. MacDiarmid, Y. W. Park, and H. Shirakawa, *J. Am. Chem. Soc.* **100**, 1013 (1978).
- ³S. A. Chen and W. G. Fang, *Macromolecules* **24**, 1242 (1991).
- ⁴D. T. McQuade, A. E. Pullen, and T. M. Swager, *Chem. Rev. (Washington, D.C.)* **100**, 2537 (2000).
- ⁵P. Novak, K. Muller, K. S. V. Santhanam, and O. Haas, *Chem. Rev. (Washington, D.C.)* **97**, 207 (1997).
- ⁶G. H. Gelinck, T. C. T. Geuns, and D. M. de Leeuw, *Appl. Phys. Lett.* **77**, 1487 (2000).
- ⁷C. J. Drury, C. M. J. Mutsaers, C. M. Hart, M. Matters, and D. M. de Leeuw, *Appl. Phys. Lett.* **73**, 108 (1998).
- ⁸F. Hide, M. A. Diaz-Garcia, B. J. Schwartz, M. R. Andersson, Q. Pei, and A. J. Heeger, *Science* **273**, 1833 (1996).
- ⁹S. Califano, *Vibrational States* (Wiley, New York, 1976).
- ¹⁰G. Zerbi, in *Advances in Infrared and Raman Spectroscopy*, edited by R. J. H. Clark and R. E. Hester (Wiley-Heyden, New York, 1984).
- ¹¹*The Optics of Thermotropic Liquid Crystals*, edited by S. Elston and R. Sambles (Taylor and Francis, London, 1998).
- ¹²S. Quillard, G. Louarn, S. Lefrant, and A. G. MacDiarmid, *Phys. Rev. B* **50**, 12496 (1994).
- ¹³L. W. Shacklette, J. F. Wolf, S. Gould, and R. H. Baughman, *J. Chem. Phys.* **88**, 3955 (1988).
- ¹⁴Y. Furukawa, F. Ueda, Y. Hyodo, I. Harada, T. Nakajima, and T. Kawagoe, *Macromolecules* **21**, 1297 (1988).
- ¹⁵B. Kostić, D. Raković, I. E. Davidova, and L. A. Gribov, *Phys. Rev. B* **45**, 728 (1992).
- ¹⁶P. Mori-Sánchez, Q. Wu, and Weitao Yang, *J. Chem. Phys.* **119**, 11001 (2003).
- ¹⁷M. van Faassen, P. L. de Boeij, R. van Leeuwen, J. A. Berger, and J. G. Snijders, *Phys. Rev. Lett.* **88**, 186401 (2002).
- ¹⁸C. J. Adam, S. J. Clark, G. J. Ackland, and J. Crain, *Phys. Rev. E* **55**, 5641 (1997).
- ¹⁹S. J. Clark, C. J. Adam, G. J. Ackland, J. White, and J. Crain, *Liq. Cryst.* **22**, 469 (1997).
- ²⁰S. J. Clark, C. J. Adam, D. J. Cleaver, G. J. Ackland, and J. Crain, *Liq. Cryst.* **22**, 477 (1997).
- ²¹S. J. Clark, G. J. Ackland, and J. Grain, *Europhys. Lett.* **44**, 578 (1998).
- ²²P. R. Tulip and S. J. Clark, *J. Chem. Phys.* **121**, 5201 (2004).
- ²³G. Zheng, S. J. Clark, P. Tulip, S. Brand, and R. A. Abram, *J. Chem. Phys.* **123**, 024904 (2005).
- ²⁴X. Gonze, *Phys. Rev. B* **55**, 10337 (1996); X. Gonze, and C. Lee, *ibid.* **55**, 10355 (1996).
- ²⁵S. Baroni, S. de Gironcoli, A. Dal Corso, and P. Giannozzi, *Rev. Mod. Phys.* **73**, 515 (2001).
- ²⁶M. Born and K. Huang, *Dynamical Theory of Crystal Lattices* (Oxford University Press, Oxford, 1954).
- ²⁷M. C. Payne, M. P. Teter, D. C. Allan, T. A. Arias, and J. D. Joannopoulos, *Rev. Mod. Phys.* **64**, 1045 (1992).
- ²⁸M. D. Segall, Philip J. D. Lindan, M. J. Probert, C. J. Pickard, P. J. Hasnip, S. J. Clark, and M. C. Payne, *J. Phys.: Condens. Matter* **14**, 2717 (2002).
- ²⁹J. P. Perdew and Y. Wang, *Phys. Rev. B* **46**, 12947 (1992).
- ³⁰L. Kleinman and D. M. Bylander, *Phys. Rev. Lett.* **48**, 1425 (1982).
- ³¹H. J. Monkhorst and J. D. Pack, *Phys. Rev. B* **13**, 5188 (1976).
- ³²L. W. Shacklette, J. F. Wolf, S. Gould, and B. H. Baughman, *J. Chem. Phys.* **88**, 3955 (1988).
- ³³J. W. Blatchford, T. L. Gustafson, and A. P. Epstein, *J. Chem. Phys.* **105**, 9214 (1996).
- ³⁴J. Hellmann, *Einführung in die Quantenchemie* (Deuticke, Leipzig, 1937); R. P. Feynman, *Phys. Rev.* **56**, 340 (1939).
- ³⁵S. Quillard, G. Louarn, S. Lefrant, and A. G. MacDiarmid, *Phys. Rev. B* **50**, 12496 (1994).
- ³⁶M. Kertesz, C. H. Choi, and S. Y. Hong, *Synth. Met.* **85**, 1073 (1997).
- ³⁷J. W. van der Horst, P. A. Robert, M. A. J. Michaels, and H. Bässler, *J. Chem. Phys.* **114**, 6950 (2001).